# Silica-Supported Au Nanoparticles Decorated by $TiO_2$: Formation, Morphology, and CO Oxidation Activity

**Anita Horváth,*,† Andrea Beck,† Antal Sárkány,† Györgyi Stefler,† Zsolt Varga,‡ Olga Geszti,§ Lajos Tóth,§ and László Guczi†**

*Department of Surface Chemistry and Catalysis and Radiation Safety Department, Institute of Isotopes, Hungarian Academy of Sciences, Post Office Box 77, H-1525 Budapest, Hungary, and Research Institute for Technical Physics and Materials Science, Konkoly Thege M. út 29/33, H-1525 Budapest, Hungary*

*Received: February 15, 2006; In Final Form: May 26, 2006*

$Au-TiO_2$ interface on silica support was aimed to be produced in a controlled way by use of Au hydrosol. In method A, the Au colloids were modified by hydrolysis of the water-soluble Ti(IV) bis(ammoniumlactato)-dihydroxide (TALH) precursor and then adsorbed on Aerosil $SiO_2$ surface. In method B, Au sol was first deposited onto the $SiO_2$ surface and then TALH was adsorbed on it. Regular and high-resolution transmission electron microscopy (TEM and HRTEM) and energy dispersive spectrometry (EDS) analysis allowed us to conclude that, in method A, gold particles were able to retain the precursor of $TiO_2$ at 1.5 wt % $TiO_2$ loading, but at 4 wt % $TiO_2$ content the promoter oxide appeared over the silica surface as well. With method B, titania was detected on silica at each $TiO_2$ concentration. In $Au-TiO_2/SiO_2$ samples, the stability of Au particles against sintering was much higher than in $Au/TiO_2$. The formation of an active $Au-TiO_2$ perimeter was proven by the greatly increased CO oxidation activity compared to that of the reference $Au/SiO_2$.

## 1. Introduction

Metal or metal oxide particles of nanometer size can be greatly affected by interactions with the support, and they possess novel catalytic properties. A recent remarkable finding in heterogeneous catalysis was the high activity of gold nanoparticles dispersed on proper supports (e.g., reducible transition metal oxides) in certain oxidation reactions. For instance, carbon monoxide can be oxidized even below room temperature.[1] Thus, supported gold seems to be a promising catalyst for the removal of CO impurity from hydrogen feedstock being used in fuel cells.[2]

It is generally agreed that high dispersion of gold and the intimate contact between the metal particles and the supporting oxide are prerequisite for excellent catalytic activity. However, there is a certain debate in the literature concerning the oxidation state of Au species.[3,4] Reducible oxides such as $TiO_2$, $Fe_2O_3$, or $CeO_2$ ensure the highest activity (active oxides), while $SiO_2$ turned to be a much less effective support (inactive oxide).[5] Concerning the mechanism of CO oxidation, CO is supposed to be weakly bonded on Au, and oxygen species are thought to be activated on the support at the perimeter of Au−oxide interface (active interface), probably at oxygen-vacancy defects.[6] The substantial role of the active interface was investigated by use of mechanical mixtures of Au colloids of 5 nm and $TiO_2$ particles of Degussa P25: although the Au particle size increased up to ∼12 nm for the sample calcined at 600 °C, its catalytic activity was as high as that of the sample prepared by the deposition precipitation method, treated the same way but having a much smaller particle size (6.7 nm).[7] This shows why the control of interface properties must be considered in studying gold catalysts.

Extensive research focusing on the controlled formation of Au-oxide interface has been pursued in our laboratory. We have studied model systems of gold/iron oxide[8,9] or gold/titania interface on $SiO_2/Si(100)$[10] and powder catalysts prepared by wet chemical method via adsorption of gold colloids on $TiO_2$[11] or $TiO_2-SiO_2$[12] supports.

When $TiO_2$ is used as a bulk support to disperse gold nanoparticles, it is obvious that an $Au-TiO_2$ interface is created. A rather challenging task is to ensure the intimate contact of these two components when $TiO_2$ is applied only as a modifier in such an amount that is comparable with the amount of Au. In this case new catalytic properties are expected to appear compared to the usual $Au/TiO_2$ system. Furthermore, an "inverse" system, viz., when the surface of Au is decorated with $TiO_2$ moieties ("localized oxide promotion" of gold), can provide new insights into the mechanism of CO oxidation on gold. There have been a few attempts to study the effect of oxide decoration on metal films. For instance, Pt(111) film was covered by $CeO_2$, and depending on the thickness of ceria layer its activity in the CO oxidation was different. The most active species was obtained when fully covered Pt was present.[13] In the literature a few studies could be found on core−shell structured nanoparticles made of titania core and gold shell.[14,15] These composite particles were prepared to study optical properties or photocatalytic activity.[16,17] Philip and co-workers[18,19] published a one-step synthesis of Au core/$TiO_2$ or $ZrO_2$ shell particles from $HAuCl_4$ and titanium isopropoxide or zirconium propoxide under reflux. The $TiO_2$ shell was suggested to form around the 50 nm sized Au particles; however, no TEM pictures were shown to verify that and only the optical properties of Au core/$ZrO_2$ shell composite were discussed in details. It seems that the application of $Au/TiO_2$ core−shell or layered structures in CO oxidation has been hardly studied yet.

* Corresponding author: phone (+36)-1-392-2534; fax (+36)-1-392-2703; e-mail ahorvath@sunserv.kfki.hu.

† Department of Surface Chemistry and Catalysis, Institute of Isotopes, HAS.

‡ Radiation Safety Department, Institute of Isotopes, HAS.

§ Research Institute for Technical Physics and Materials Science.

10.1021/jp060977b CCC: $33.50 
Published on Web 07/20/2006

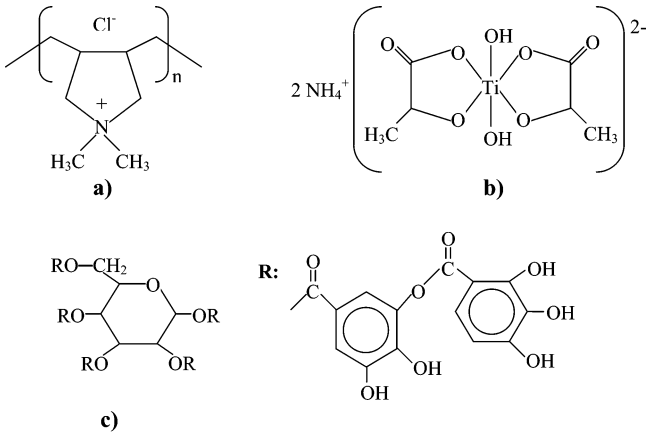


**Figure 1.** Structures of (a) PDDA, (b) TALH, and (c) tannic acid.

In the present work our results on the structure and CO oxidation activity of $TiO_2$-decorated $Au/SiO_2$ catalysts are shown. Our aim was to ensure the intimate contact of nanosize $TiO_2$ and gold colloids in a so-called "inverse system" (when $TiO_2$ is on top of Au). By use of gold sols, titania coverage on/around the Au nanoparticles was produced on $SiO_2$ support. The different catalytic activity of the $SiO_2$-supported samples, depending on the Ti loading, points to the existence and the importance of active interface between Au and the nanosize $TiO_2$ of different morphology.

## 2. Experimental Section

**2.1. Catalyst Preparation.** Aqueous solutions of $HAuCl_4 \cdot 3H_2O$ (Aldrich); poly(diallyldimethylammonium) chloride (PDDA), 20 wt % in water (Aldrich), (Figure 1a); Ti(IV) bis-(ammoniumlactato)dihydroxide (TALH), 50 wt % in water (Aldrich) (Figure 1b); tannic acid (Aldrich) (Figure 1c); sodium citrate (Aldrich); and commercial silica (Aerosil 200, Degussa) or titania(Eurotitania, Tioxide International) supports were used in the preparations.

Gold hydrosol with an average particle size of about 18 nm was produced by the conventional citrate method: $Au^{3+}$ ions were reduced with sodium citrate in aqueous solution at 95 °C under reflux for 1 h ($c_{Au}$ in sol = 0.25 mM). The preparation of gold sol with $d_{Au} \sim 6$ nm is described elsewhere.[11] Briefly, $HAuCl_4$ was reduced by a mixture of tannic acid and sodium citrate at 60 °C and left at that temperature for 30 min under stirring. The red color of the sol evidenced the reduction of $Au^{3+}$ ions.

The above sols were used in the next steps, when the Ti component was introduced in two different ways. The main steps of the two preparations are shown in Scheme 1. In preparation method A, a calculated amount of aqueous solution of TALH was added to the sols at room temperature (to give Ti/Au = 0.2−11) under stirring for 1 h, and then the temperature was increased to 60 °C within 1 h and kept there for 4 h (to hydrolyze TALH). Finally, the sol was cooled to room temperature and left for overnight under stirring. No color change was observed during the procedure of Ti(IV) addition, and the sol was stable on the following day as well. Then, the adsorption of Ti-containing Au sols (composite sol) onto Aerosil $SiO_2$ was accomplished with the aid of PDDA. Without this additive, the adsorption of the sols on silica could not take place. Certain amount of PDDA (depending on the actual sol, usually 1.5−1.7 mL of 0.08 wt % aqueous PDDA solution per 100 mg of $SiO_2$) was preadsorbed on Aerosil under stirring at room temperature. Next, the pure Au or the composite sol was added to the silica suspension and the white color of silica changed to red or reddish purple as a sign of the successful adsorption. In some cases, an additional amount of PDDA was necessary to facilitate the adsorption of the composite sol. The suspension was stirred vigorously at room temperature for about 1 h, and then the solid was separated by filtration, washed thoroughly with water, and dried for 2 days at 65 °C. Thus, catalysts with different $TiO_2$ content were produced with comparable Au loading. As references, ~2 wt % Au/Aerosil $SiO_2$ ($Au/SiO_2$) and ~2 wt % Au/Eurotitania $TiO_2$ were prepared ($Au/TiO_2$) in the same way without addition of Ti precursor. Since Au sintering on bulk $TiO_2$ support was significant after calcination at 450 °C (catalyst pretreatment before CO oxidation reaction), Au sol with smaller initial particle size was prepared by increasing the tannic acid concentration 4 times. The sol thus prepared was composed of Au particles of ~5 nm that were adsorbed on $TiO_2$.

In preparation method B, the $Au/SiO_2$ reference sample was further processed. The dried sample was mixed with the appropriate amount of TALH solution at 50 °C for 40 min, then the temperature was raised to 60−65 °C and the water was allowed to evaporate (it took usually 4−5 h). Finally, the Ti-loaded $Au/SiO_2$ samples were dried for 2 days at 60−65 °C.

The Aerosil-supported samples prepared by method A are denoted for instance by AS6Ti0.2 and AS18Ti1.3, respectively, where the first digits (6 or 18) refer to the approximate Au particle size in the parent gold sol and the digits at the end indicate the $TiO_2$ content in weight percent. The samples produced by method B are labeled in the same way but with starting letter B. For the sake of correct comparison, a "blank" $TiO_2$-modified $SiO_2$ was prepared; the $TiO_2$ modification was done by method B on the Aerosil after PDDA preadsorption and drying.

**2.2. Determination of Au and Ti Content.** The Ti and Au content of the samples were determined on a double-focusing inductively coupled plasma mass spectrometer (ICP-MS, ELEMENT2). All measurements were made with a Scott-type spray chamber operating at room temperature and a Meinhard concentric nebulizer. Dried catalyst sample of 1−8 mg was accurately weighed into a high-purity poly-propylene vial. The dissolution was carried out using 1 mL of $HNO_3$, 3 mL of HCl, and 2 mL of HF acid mixture. The sample was heated up to 80 °C in water bath for 10 min and cooled down to room temperature afterwards. No visible residue was left after the dissolution. Then the sample was filled up to 20 g with high-purity water. All dilutions were carried out by weight measurements. Subsequently, 1 mL aliquot of sample was measured into a PFA beaker and 1 mL of $HNO_3$ and 3 mL of HCl were added and evaporated to almost complete dryness to remove excess HF. Finally, the samples were transferred into PP vials using high-purity water. Further dilutions were made using 2% (w/w) $HNO_3$/2% (w/w) HCl solution. 1 ng g-1 Rh internal standard was used before the ICP−MS analysis.

**2.3. TEM Measurements.** The distribution of Au and Ti and the size of gold particles were studied on a Philips CM20 transmission electron microscope (TEM) operating at 200 kV equipped with energy-dispersive spectrometer (EDS) for electron probe microanalysis. The aqueous suspensions of the $Au-TiO_2/SiO_2$ samples were dropped on a carbon-coated grid, and after evaporation of water, electron micrographs of the particles were taken. The gold particle size distribution was obtained by measuring the diameter of equiaxial metal particles. Two of the samples were investigated also in a JEOL 3010 high-resolution

**SCHEME 1: Main Steps of Preparation with the Suggested Structures and Interactions: (a) Method A and (b) Method B**

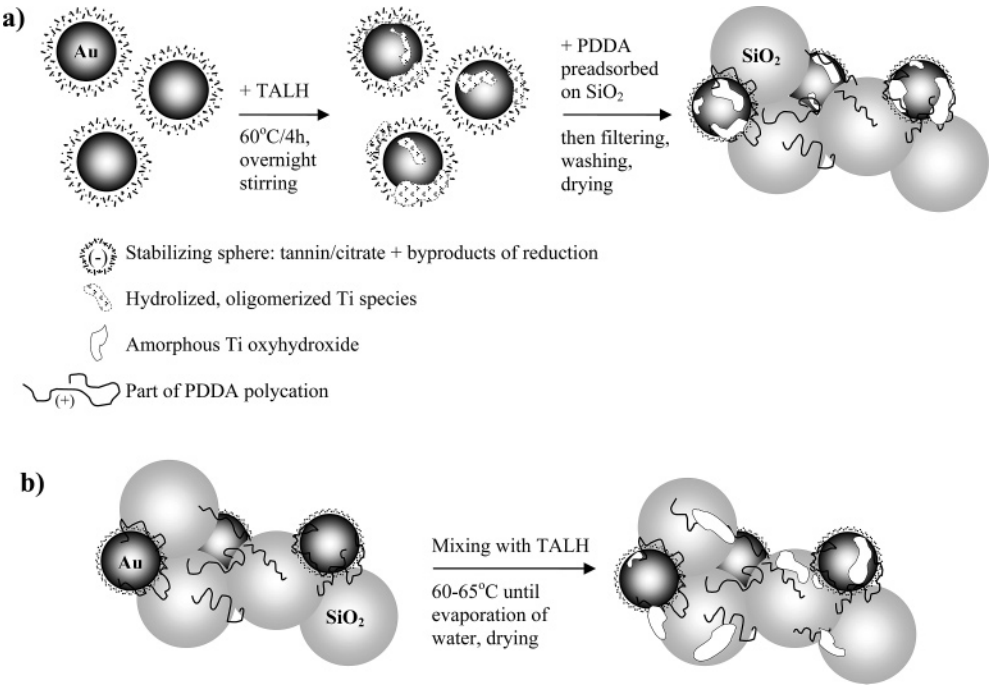


**TABLE 1: Metal Loading and Au Particle Size in the Sol and in the Supported Samples after Calcination and Catalytic Run**

| sample | Au content (wt %) | $TiO_2$ content (wt %) | Ti/Au | $d_{Au}$ (nm) | $d_{Au}$ in sol[a] (nm) |
|---|---|---|---|---|---|
| AS6Ti0.2 | 2.0 | 0.2 | 0.2 | | 6.5 |
| AS6Ti0.8 | 1.8 | 0.8 | 1.0 | | 6.5 |
| AS6Ti1.5 | 1.9 | 1.5 | 1.9 | $7.2 \pm 1.5$[b] | $6.5 \pm 1.5$ |
| BS6Ti1.0 | 1.8 | 1.0 | 1.4 | | $6.5 \pm 1.5$ |
| AS18Ti1.3 | 1.4 | 1.3 | 2.3 | | $18.2 \pm 1.6$ |
| AS6Ti3.9 | 1.9 | 3.9 | 5.0 | $6.6 \pm 2.0$[b] | 6.5 |
| BS6Ti3.9 | 1.8 | 3.9 | 4.3 | $6.9 \pm 1.5$[b] | 6.5 |
| BS6Ti4.2[c] | 2.2 | 4.2 | 5.6 | | 6.5 |
| AS6Ti6.5 | 1.4 | 6.5 | 11.1 | | 6.5 |
| $Au/SiO_2$ | 2[d] | | | $6.7 \pm 1.8$[e] | 6.5 |
| $Au/TiO_2$ | 1.8 | | | $11 \pm 6.8$[b] | $4.8 \pm 1.8$ |

[a] With the exception of S18, all the Au sols were prepared under the same conditions. [b] After calcination at 450 °C. [c] Repeated synthesis of BS6Ti3.9. [d] Nominal Au loading. [e] After calcination at 350 °C.

transmission electron microscope (HRTEM) at 300 kV accelerating voltage with resolving power of 0.17 nm.

**2.4. Catalytic Tests.** CO oxidation was measured at atmospheric pressure in a plug flow reactor connected to a QMS type Pfeiffer TSU 071 E. Catalyst of 30 mg was in situ calcined at 350 or 450 °C in 20% $O_2$ in He mixture for 1 h (10 °C/min heating rate, 30 mL/min gas flow). Temperature-programmed reaction was performed with a gas flow of 0.54% CO and 9.1% $O_2$ in He with 4 °C/min ramp rate. The conversion was calculated on the basis of the $CO_2$ production.

## 3. Results and Discussion

**3.1. Formation of Au−$TiO_2$ Nanostructures on Silica Support.** The gold sol preparation either by citrate only or by citrate and tannic acid reduction has given nicely reproducible particle size, $d_{Au} = 18$ and 6.5 nm, respectively. It was also ascertained that the sol adsorption step onto the support did not change the original particle size. Table 1 shows the Au and Ti loading data and the particle size of the most representative samples after calcination and catalytic tests. It is clearly seen that in preparation method A both the Au and the Ti components were successfully attached to the $SiO_2$. In preparation method B when first the $Au/SiO_2$ reference catalyst was prepared, the success of Ti introduction is obviously successful, since after the evaporation of water from the TALH solution the Ti species should remain on the catalyst. Although Au content differs to some extent for each sample, the samples are comparable because the catalytic activity is not governed directly by Au loading (vide infra).

It is well-known that preparation of active Au catalysts fails by a deposition−precipitation method over $SiO_2$ support; for $Au/SiO_2$, vapor deposition is a more successful technique.[20] When gold sols are prepared from $HAuCl_4$ by citrate/tannic acid reduction, the gold nanoparticles are expected to be negatively charged; therefore, the adsorption of the metal particles does not occur on $SiO_2$ due to charge repulsion between the stabilized metal particles and the silica surface charged negatively above pH = 2−3. In our case the problem of the absence of attraction could be overcome with the aid of PDDA. Since PDDA is a polycation, a monolayer coverage is expected to form spontaneously on negatively charged substrates such as silica, causing charge neutralization followed by charge reversal (positive surface charge) upon increasing the polymer bulk concentration.[21−23] The ionic strength of the medium and the nonelectrostatic surface affinity of the polymer have a great influence on the adsorption step.[24,25] The idea of using PDDA as a "binding agent" for our gold sols is originated from our earlier studies when PDDA was used as stabilizer for Pd colloids.[26] By increasing the pH, higher metal loading could be achieved on $SiO_2$ support, supposedly because of the increased adsorption of the polycation and thus the metal particles on the more negative silica surface. Another advantage of applying PDDA in the present work was that, after the adsorption of gold colloids, the Aerosil silica could be filtered and washed, since large enough aggregates of the individual $SiO_2$ particles of 12 nm were formed. This is in accordance with the work of

Jacobasch and co-workers.[27] They investigated PDDA adsorption on silica surfaces and assumed that a patch of a positive polymer charge on a silica particle could interact with a patch of negative particle charge on the other one, causing flocculation of the silica particles. In our case the preadsorption of PDDA on $SiO_2$ was expected to provide a positively charged surface for the gold colloids. It is worth mentioning that there was an optimum amount of PDDA, depending on the sol composition that facilitated the adsorption of Au particles. At high concentration of the polycation there may be free positively charged PDDA chains not only on the silica but in the liquid phase and around the Au particles as well, causing the adsorption step to fail. Thus, by trial and error we could achieve a uniform distribution of Au particles through the support. Similarly to our adsorption conditions, Kekkonen and Stenius[28] applied PDDA to coat silica surface and provide a sufficiently positive layer for the adsorption of negatively charged aqueous dispersion of wood resin droplets. Although the adsorption of gold nanoparticles was accomplished on $SiO_2$, the exact conditions of the adsorption and their effect on the adsorption kinetics are still unknown and must be studied in the future via colloid chemical methods.

The situation is further complicated by the application of the water-soluble titanium precursor TALH that is partially dissociated into an anion and a $NH_4^+$ cation.[29] The advantage of TALH over the usual titania precursors such as alkoxides is its relative high resistance toward hydrolysis. If titanium alkoxides were introduced into the aqueous sol, the titanium hydroxide would have immediately precipitated. TALH was used for preparation of titania thin films on silicon, glass, and plastic substrates[30] or for production of titania coatings on silica particles. In the latter case, the silica surface was observed to be unevenly covered by $TiO_2$ particles of 3 nm.[31] Willig and co-workers[29] investigated the thermohydrolysis of TALH, producing anatase nanocrystals. During the course of thermohydrolysis the replacement of the chelating ligands by OH was suggested, followed by condensation and branching steps resulting in three-dimensional clusters and then, via the rearrangement of Ti and O atoms, anatase nanocrystals. In our case a relatively mild hydrolysis condition was set (at 60 °C) for TALH in the presence of gold sol (preparation method A) or in the suspension of $Au/SiO_2$ (preparation method B) and there was no sign of color change or aggregation even after overnight stirring. When higher temperature (80−90 °C) was applied, opacity and/or destabilization of gold sol occurred. Concerning preparation method A, adsorption of the Au particles and the probably partially hydrolyzed TALH was done with the application of PDDA preadsorbed on Aerosil silica. In some cases, addition of further PDDA was necessary after the sol had been added to the suspension of silica to reach a successful adsorption.

Concerning the components present in our system and the information listed above, the scenario shown in Scheme 1 can be suggested for the formation of $Au-TiO_2$ nanostructures on silica support. First we consider preparation method A. Au colloids surrounded by tannic acid and citrate (and the byproducts of reduction) must have a negative surface charge. Tannic acid, the digalloyl ester of glucose (see Figure 1c), belongs to the group of hydrolyzable tannins.[32] The $COO^-$ groups formed by the partial hydrolysis of tannic acid are thought to be involved in the stabilization of Au. Similar interaction between hydrous iron oxide particles and tannic acid was suggested by Horton and co-workers.[33] The next step in the preparation process is the addition of TALH. We are not able to declare in what form TALH is present at the end of overnight stirring, but we suppose the formation of Ti-oxy-hydroxide oligomer species by the partial hydrolysis of TALH. Since Ti(IV) ions in aqueous solution are able to coordinate to phenolic oxygen groups of tannin[34] and to citrate ions,[35] we assume that hydrolyzed Ti species likely having positive surface charge[36] are mainly located around the gold cores. In addition, Au particles must serve as nucleation sites for the condensation of Ti species. In the sol adsorption step, PDDA binds the gold particles covered by partially hydrolyzed tannic acid and Ti species to the silica surface, since association of both with positively charged polyelectrolytes such as PDDA can be expected.[37−40]

In the case of preparation method B, the gold nanoparticles are located already on silica when the partial hydrolysis of TALH takes place. Thus, TALH and other titania species may be deposited not only on Au but also on silica. Drying and the subsequent calcination in air remove the carbonaceous deposits from the catalysts and transform all Ti species into $TiO_2$ (or $TiO_x$).

**3.2. Structure of the Catalysts: Particle Size and Distribution of Ti Species.** From the particle size data presented in Table 1, it is clearly seen that Ti deposition does not cause any obvious increase in Au diameter. On one hand, in the case of AS6Ti1.5 sample, if all Ti present in the sample were located only on the gold particles, a maximum of $10 \times 0.35$ nm $= 3.5$ nm thick $TiO_2$ layer would form on Au (because the $Ti_{total}/Au_{surface}$ ratio is approximately 10). On the other hand, if crystalline anatase covered the entire silica surface, 22 wt % $TiO_2$ loading would be necessary to reach a monolayer coverage in the case of 200 $m^2/g$ Aerosil,[41] and we have at the most only 6.5 wt %.

Detection of the titania phase by X-ray diffraction (XRD) technique can be excluded[42] because of the high $TiO_2$ dispersion and low loading. TEM together with EDS might provide evidence of titania location as the following literature search on this topic suggests. Haruta and co-workers[43] modified a nonporous silica by impregnation with titanyl acetylacetonate (Ti/Si = 2/100), and after calcination at 400 °C most of the titanium oxide was amorphous, while after the titania-modified silica was calcined at 1000 °C many titanium oxide crystals were seen in the TEM images. According to Peden and co-workers,[41] the dispersed $TiO_2$ layer on fumed silica and silica spheres was produced from titanium alkoxides, but upon taking TEM images, there was no evidence for the presence of titania coatings on the Cabosil supports, while for silica spheres only a pronounced contrast could be observed. In another study,[44] silica spheres of 1050 nm were covered with an Ag shell of about 75 nm on which tetra-*n*-butyl titanate was deposited and hydrolyzed, forming an outer titania shell of 70 nm thickness. After the deposition of titania, the only remarkable difference was a significant decrease in the surface roughness of the $Ag/SiO_2$ spheres shown by SEM and TEM. Furthermore,[45] $Au-TiO_2$ composite thin film on glass surface was prepared by a sol−gel process containing Au film of 14−22 nm thickness, but anatase titania appeared only after calcination at 500 °C.

A TEM image taken of S6Ti1.5 sol (not shown) did not reveal the presence of $TiO_2$ particles in the sol; only Au colloids could be seen. Figure 2 depicts the TEM micrographs of samples AS6Ti1.5 (Figure 2a) and BS6Ti1.0 (Figure 2b) along with the corresponding EDS data taken at many different points of the samples (Figure 2c,d). Figure 3 shows the same information for AS6Ti3.9 and BS6Ti3.9. There is no sign of titania particles in any of our TEM pictures; only EDS proves the presence of Ti in the catalysts. Using EDS collected from 20 to 50 nm diameter spots, we detected some differences between the two preparation methods, especially at lower Ti contents (Figure 2)

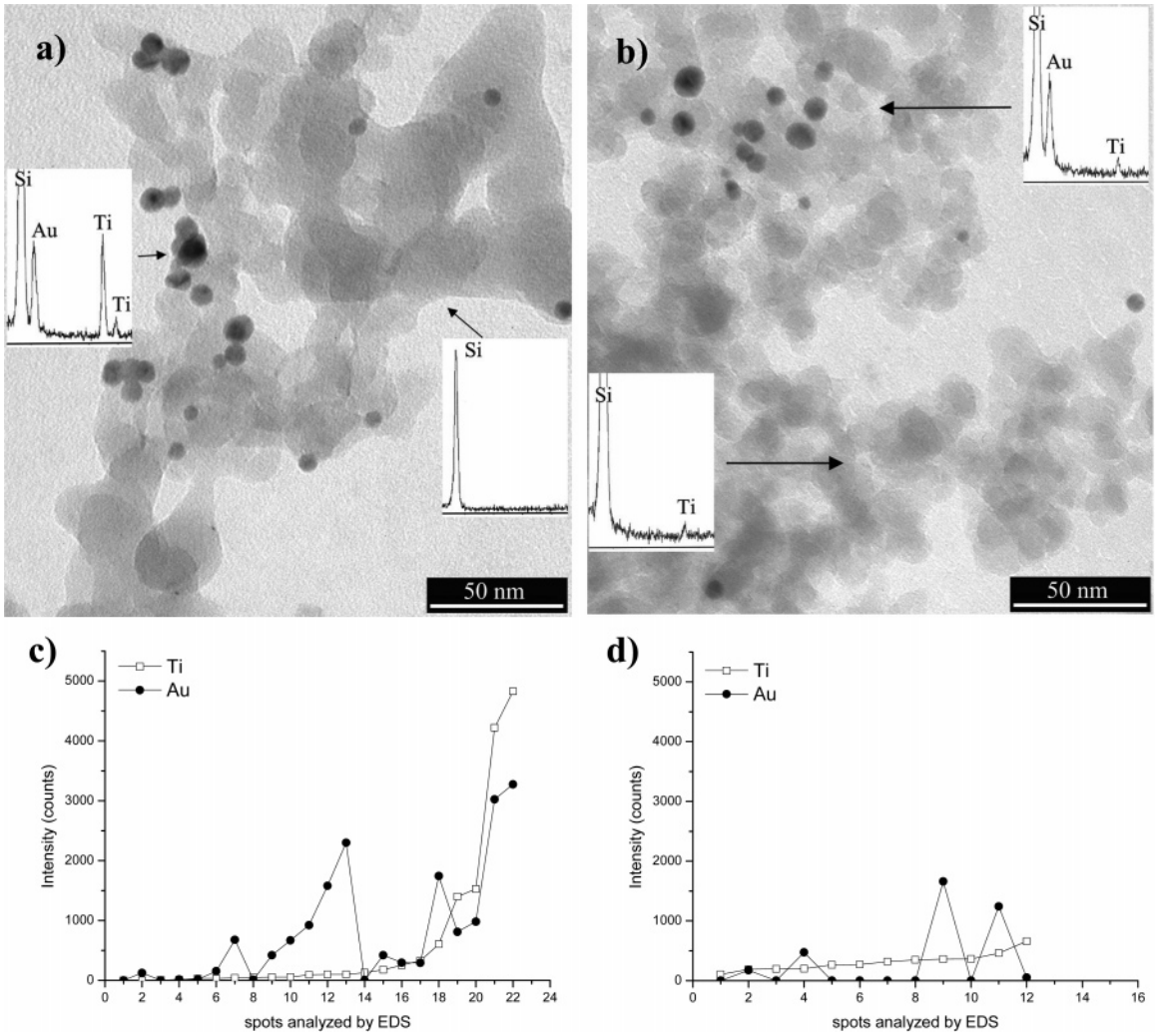


**Figure 2.** TEM images taken after calcination at 450 °C and catalytic reaction on (a) AS6Ti1.5 and (b) BS6Ti1.0, and EDS results on (c) AS6Ti1.5 and (d) BS6Ti1.0.

concerning the location of Ti. In the case of method A at 1.5 wt % Ti (see Figure 2c), where the Au particles were not seen, the analysis did not reveal the presence of Ti. Focusing the electron beam on gold particles, we observed low Ti (spots 7−14) or high Ti intensity (spots 15−24). It appears that Ti is present mainly at the sites where Au particles appear. It means that a specific attraction, ensured by the stabilizing sphere of tannic acid and citrate, dictates the bonding of TALH and/or the hydrolyzed and polymerized titanium species to Au particles already in liquid phase. When TALH is added to the preformed $Au/SiO_2$ sample (method B, 1 wt % $TiO_2$; see Figure 2d), Ti could be detected on both silica and gold. We may, therefore, suggest that for preparation A the Ti is enriched on/around gold nanoparticles (that is seen in Figure 2c and Figure 3c); that is, with increasing Au counts there is an increasing level of Ti counts. One has to note that in the case of 3.9 wt % $TiO_2$ Ti signal could be observed at certain spots of the sample without detecting Au as shown in Figure 3c. Consequently, adsorption of Ti species on $SiO_2$ cannot be excluded.

To further clarify the problem of titania location, two samples prepared by method A were chosen for HRTEM investigations. The high-resolution TEM micrographs of AS6Ti1.5 and AS6Ti3.9 are shown in Figures 4 and 5, respectively. A single Au particle of AS6Ti1.5 is seen in Figure 4a with pentagonal twin boundaries (marked with arrows) to evidence that the individual Au colloids formed in the course of liquid phase reduction have many defect sites and dislocations that can differently behave in the catalytic run. Figure 4 panels b and c suggest the presence of $TiO_x$ in intimate contact with the Au surface. A few layers thick shell can be observed partly covering the Au particle in Figure 4b. The spacing between the layers (0.35 nm) corresponds to the (101) interplanar spacing of anatase (JCPDS 21-1272). Figure 4c depicts Au nanoparticles surrounded by a 1−2 nm thick layer with structure differing from that of amorphous $SiO_2$ that is shown on patterns obtained by Fourier transform (FFT) inserted in Figure 4c. This shell structure can be attributed to the metastable $\beta$-$TiO_2$ phase (JCPDS 35-0088), since the spacing between the layers $d = 0.57$ nm is close to the spacing of (200) plane of $\beta$-$TiO_2$ ($d = 0.579$ nm). This type of titania can be formed after calcining of amorphous $TiO_2$ at 450−600 °C, and it may coexist with the more common anatase phase.[46] Calcination of titanate nanoribbons that formed by hydrothermal treatment of $TiO_2$ produced also $\beta$-$TiO_2$ phase.[47] The HRTEM of AS6Ti1.5 sample thus evidences a $TiO_2$ overlayer on Au that is a few layers thick (but according to EDS measurements may not homogeneously cover all Au particles) and comprises partially ordered anatase and $\beta$-$TiO_2$ phases.

In the case of higher Ti loading (3.9 wt % Ti), there was definite proof for the presence of two types of crystalline overlayer at several points of the amorphous $SiO_2$ and on the crystalline Au particles (see Figure 5). The interplanar spacing

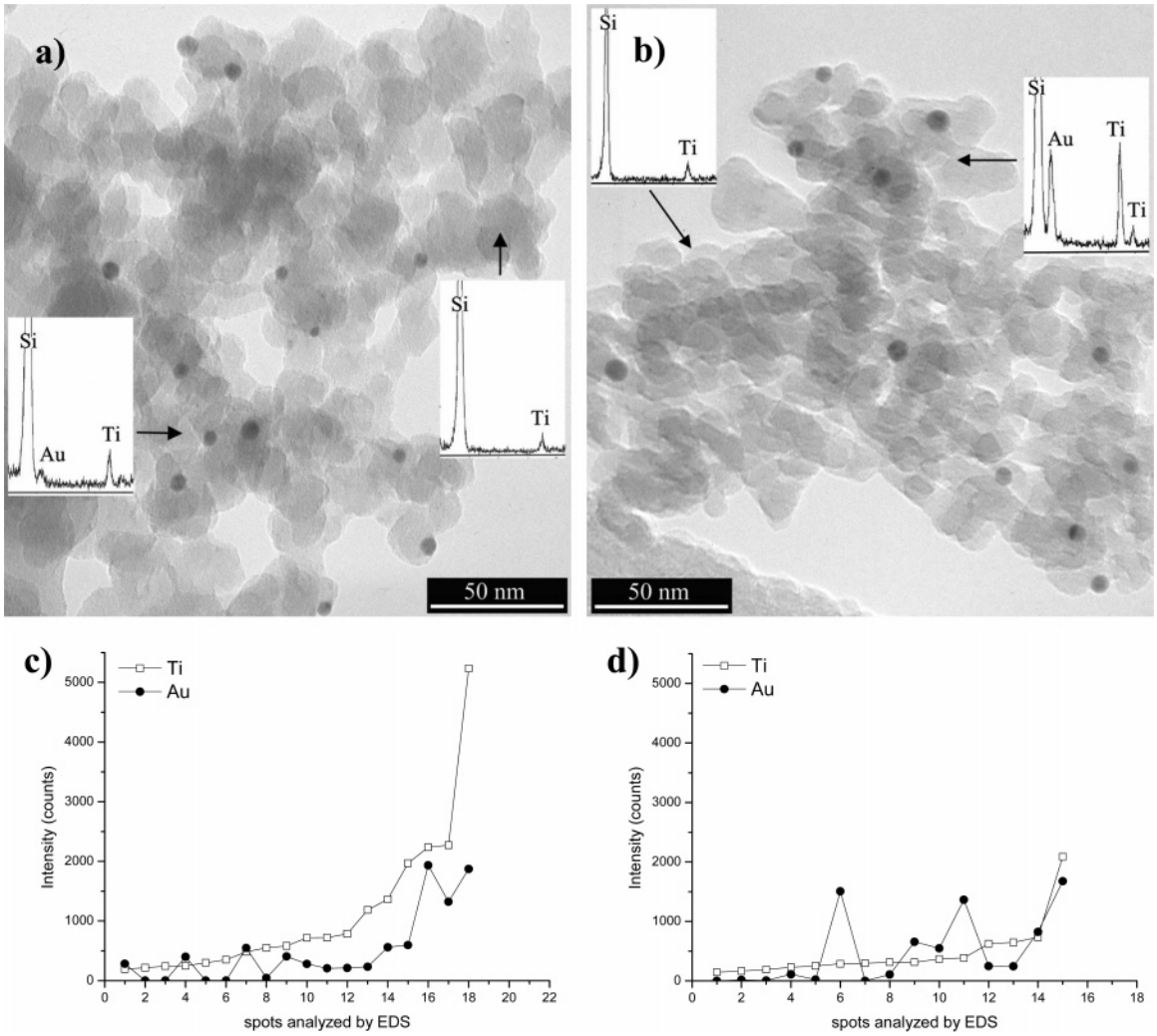


**Figure 3.** TEM images taken after calcination at 450 °C and catalytic reaction on (a) AS6Ti3.9 and (b) BS6Ti3.9, and EDS results on (c) AS6Ti3.9 and (d) BS6Ti3.9.

for one type of crystalline material is that of (101) plane of anatase ($d = 0.35$ nm) shown by the Fourier transform inset in the figure. The other titania phase has a lattice spacing of $d = 0.57$ nm that is assigned to the (200) plane of $\beta$-$TiO_2$ phase again. $TiO_2$ fringes are seen on the Au particle as well with some dislocations. According to these results, in the case of ~4 wt % $TiO_2$ content a very thin crystalline titania overlayer/sheet or islands of titania were formed on the Au particles and also on silica after calcination at 450 °C. Thus, we can accept the existence of surface $TiO_2$ that covers and surrounds the Au particles, providing an increased Au−$TiO_2$ interfacial area.

Concerning the stability of particle size, we can draw up the following statements. The size of the Au particles in Au−$TiO_2$/$SiO_2$ systems was hardly affected by calcination (Table 1) and the size distribution is relatively narrow (see Figure 6). The particle size is also stable in the case of Au/$SiO_2$, but it greatly increases and the size distribution becomes rather heterogeneous in the case of Au/$TiO_2$. For the Au/$TiO_2$ preparation, we made some efforts to use a parent Au sol with smaller particle size ($d = 5$ nm instead of 6 nm used for the other samples) and applied a slower temperature ramp up to 450 °C during the pretreatment (see Figure 7), but the sintering could not be avoided and the final size was $d = 11$ nm. Tsubota and co-wiorkers[48] also observed that the size of Au particles after 400 °C calcination increased on a pure titania support; however, it did not change in the case of a titania-coated silica aerogel.

**3.3. Catalytic Properties.** Although Wachs and co-workers[49] suggested an increased oxidizing potential in methanol oxidation and a decreased acidity of the Ti cations when dispersed on silica support, in our case the blank $TiO_2$/$SiO_2$ sample showed very low oxidation activity: CO oxidation started at 300 °C, and up to 450 °C only 17% conversion was achieved.

The catalytic reaction proved to be the most sensitive test to show the intimate contact of nanosized $TiO_2$ and Au phases in the samples containing both components. The activity of the sample with $TiO_2$ content as low as 0.2 wt % was already higher than that of Au/$SiO_2$. Figure 8 shows that as the Ti content increased the activity greatly increased, viz., the temperature of 50% CO conversion was strongly lowered until it reached a broad minimum. Delgass and co-workers[42] have arrived at a somewhat similar conclusion by studying Au−$TiO_2$ nanoclusters supported on $SiO_2$ prepared by distributed arc cluster source technique. Their catalytic activity in propylene epoxidation followed a maximum-type curve depending on the composition: the sample with Ti/Au = 0.5 was the most active one, while at higher Ti contents the gold surface was largely covered by $TiO_2$ phase, and thus the activity dropped. In Figure 8 it can also be seen that the activity after 350 °C calcination was usually lower than that after 450 °C for each sample, suggesting a slightly unstable structure of Au−$TiO_2$ units (the transformation of amorphous $TiO_x$ to crystalline forms) and/or the presence of organic residues left over the samples calcined at 350 °C.

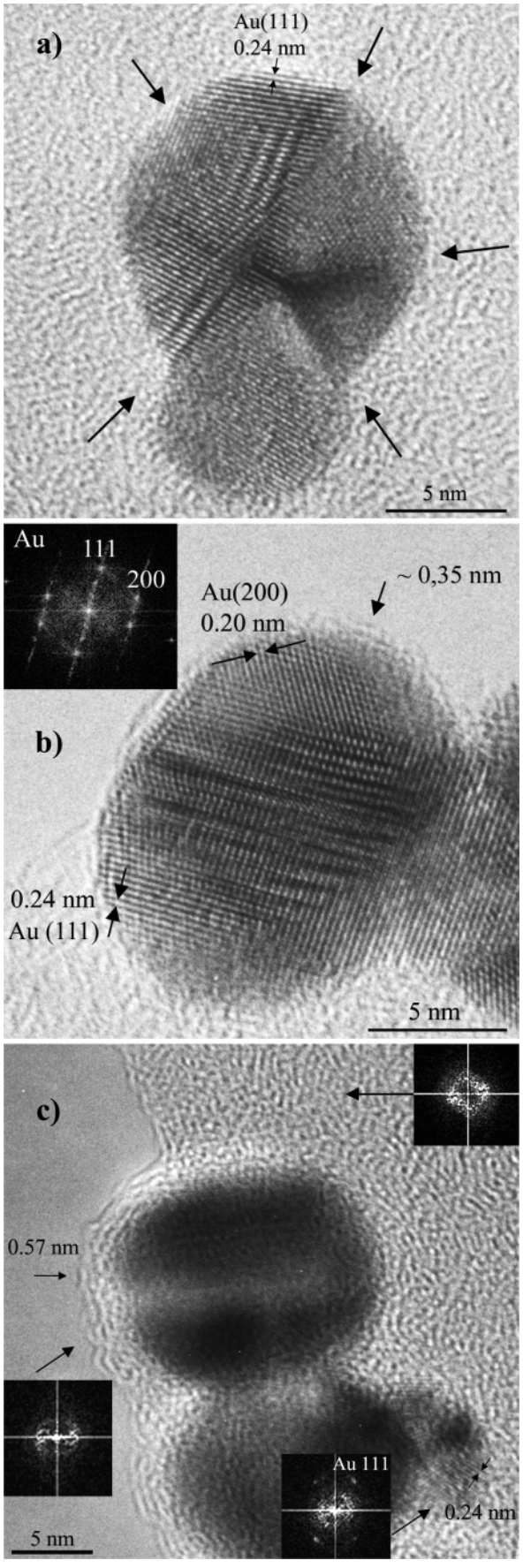


**Figure 4.** HRTEM picture of AS6Ti1.5 after calcination at 450 °C and catalytic run: (a) Au particle with twin boundaries; (b) Au particle covered by titania patches of anatase structure; (c) Au particles covered by $\beta$-$TiO_2$ phase

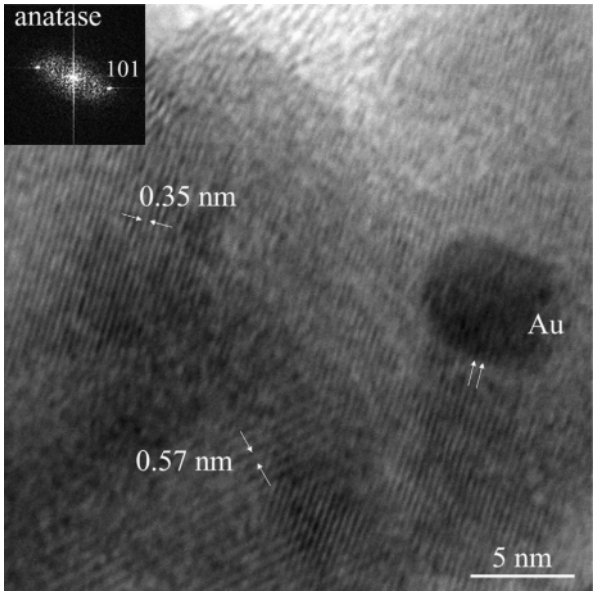


**Figure 5.** HRTEM picture of AS6Ti3.9 after calcination at 450 °C and catalytic run.

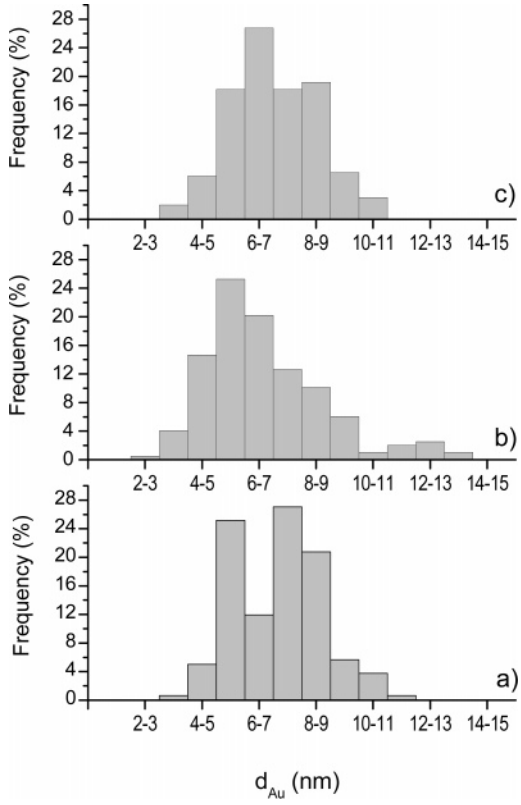


**Figure 6.** Au particle size distribution of (a) AS6Ti1.5, (b) AS6Ti3.9, and (c) BS6Ti3.9 after calcination at 450 °C and catalytic run.

Figure 9 shows the CO conversion curves for the most active samples prepared by methods A and B along with the curve of $Au/TiO_2$. The high activity of the samples containing a small amount of titania suggests that as large active $Au-TiO_2$ interface as in $Au/TiO_2$ was achieved, although the difference in Au particle size (see Table 1) and structural differences between the two types of titania should be taken into account. The very thin layer or the decorating patches of nanosize $TiO_2$ in contact with gold must have different oxidizing properties than bulk $TiO_2$. Iwasawa and co-workers,[50,51] using as-precipitated

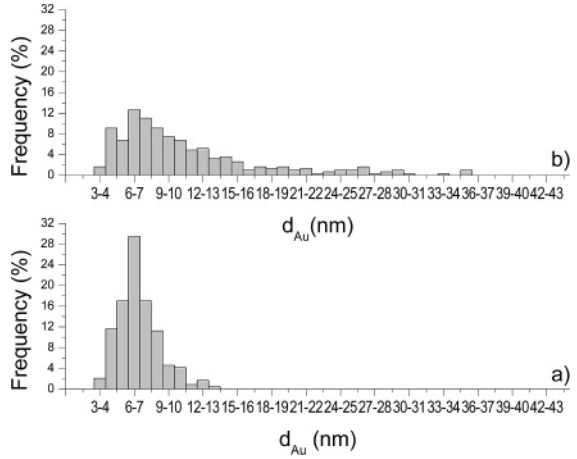


**Figure 7.** Au particle size distribution of (a) $Au/SiO_2$ after calcination at 350 °C and catalytic run and (b) $Au/TiO_2$ after calcination at 450 °C and catalytic run.

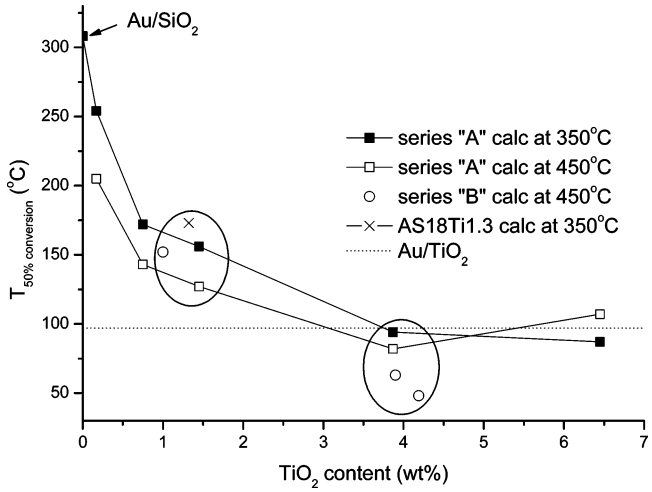


**Figure 8.** Temperature of 50% CO conversion versus $TiO_2$ content.

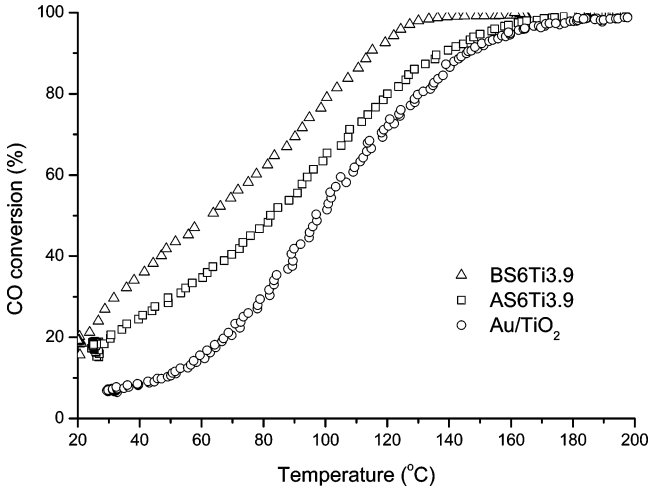


**Figure 9.** CO conversion on the most active samples compared to $Au/TiO_2$ (pretreatment: calcination at 450 °C).

$Ti(OH)_4$ impregnated with Au-phosphine complex and calcined at 400 °C, observed different adsorption properties of $O_2$ for the hydroxide-based gold sample compared to a traditional $TiO_2$-supported gold catalyst that most probably contributed to the increased CO oxidation activity.

At first glance the similar activity of BS6Ti3.9 compared to AS6Ti3.9 is somewhat surprising. If all the Ti evenly covered the catalyst surface, there would be a very low coverage of $TiO_x$ on gold parts, and consequently, lower activity should be observed. The fact that method B results in catalyst with similar activity as method A suggests that the deposition of Ti species during method B might also be governed by the interactions between the partially hydrolyzed TALH, tannic acid, and PDDA and results in similar morphology as method A. Remember that the calcination pretreatment at 450 °C may diminish the structural differences between the samples prepared by methods A and B. All in all, the formation of a large active $Au-TiO_2$ interface in $Au-TiO_2/SiO_2$ systems with low $TiO_2$ concentration is obvious.

## 4. Conclusions

Two colloid chemical preparation routes for synthesis of $Au-TiO_2/SiO_2$ catalysts have been described. In method A, Au sol was decorated by titania precursor in the liquid phase by slow hydrolysis of TALH and the composite sol was adsorbed onto Aerosil surface by means of PDDA polycation. In method B, the Au sol was adsorbed on $SiO_2$ surface by use of PDDA and then the $Au/SiO_2$ was decorated with titania precursor by adsorbing/hydrolyzing TALH.

At low $TiO_2$ concentration (1−1.5 wt %), TEM and EDS measurements provide evidence that $TiO_x$ is located on or around Au particles for method A, while for method B titania can be detected also on the support. It was observed that at higher $TiO_2$ loading (∼4 wt %) Ti appears both on the $SiO_2$ support and in Au particles. With increasing $TiO_2$ concentration, CO oxidation activity was enhanced, and at 4 wt % $TiO_2$ similar activity was reached as in the case of $Au/TiO_2$ reference catalyst, proving the formation of a large active $Au-TiO_2$ interface. As revealed by TEM, $Au/TiO_2$ reference sample after calcination at 450 °C showed particle coalescence and growth whereas over $Au-TiO_2/SiO_2$ samples the size of Au particles was not affected.

**Acknowledgment.** We are indebted to National Science and Research Fund (OTKA) Grants T-049564 and F-62481 and the COST D15 Program D15/0016/2001.

## References and Notes

(1) Haruta, M. *Catal. Today* **1997**, *36*, 153−166.
(2) Ghenciu, A. F. *Curr. Opin. Solid State Mater. Sci.* **2002**, *6*, 389−399.
(3) Fu, Q.; Deng, W.; Saltsburg, H.; Flytzani-Stephanopoulos, M. *Appl. Catal., B* **2005**, *56*, 57−68.
(4) Bond, G. C.; Thompson, D. T. *Gold Bull.* **2000**, *33*, 41−51.
(5) Schimpf, S.; Lucas, M.; Mohr, C.; Rodemerck, U.; Brückner, A.; Radnik, J.; Hofmeister, H.; Claus, P. *Catal. Today* **2002**, *72*, 63−78.
(6) Boccuzzi, F.; Chiorino, A.; Manzoli, M.; Lu, P.; Akita, T.; Ichikawa, S.; Haruta, M. *J. Catal.* **2001**, *202*, 256−267.
(7) Tsubota, S.; Nakamura, T.; Tanaka, K.; Haruta, M. *Catal. Lett.* **1998**, *56*, 131−135.
(8) Guczi, L.; Petõ, G.; Beck, A.; Frey, K.; Geszti, O.; Molnár, G.; Daróczi, C. *J. Am. Chem. Soc.* **2003**, *125*, 4332−4337.
(9) Guczi, L.; Frey, K.; Beck, A.; Petõ, G.; Daróczi, Cs.; Kruse, N.; Chenakin, S. *Appl. Catal. A* **2005**, *291*, 116−125.
(10) Frey, K.; Beck, A.; Petõ, G.; Molnár, G.; Geszti, O.; Guczi, L. *Catal. Commun.* **2005**, *7*, 64−67.
(11) Guczi, L.; Beck, A.; Horváth, A.; Koppány, Z.; Stefler, G.; Frey, K.; Sajo, I.; Geszti, O.; Bazin, D.; Lynch, J. *J. Mol. Catal.* **2003**, 204−205, 545−552.
(12) Venezia, A. M.; Liotta, F. L.; Pantaleo, G.; Beck, A.; Horváth, A.; Geszti, O.; Kocsonya, A.; Guczi, L. Effect of Ti(IV) loading on CO oxidation activity of gold on titania doped silica. *Appl. Catal.* (in press).
(13) Hardacre, C.; Ormerod, R. M.; Lambert, R. M. *J. Phys. Chem.* **1994**, *98*, 10901−10905.
(14) Wang, C.; Liu, C.; Chen, J.; Shen, T. *J. Colloid Interface Sci.* **1997**, *191*, 464−470.
(15) Zhao, S.; Chen, S.; Wang, S.; Quan, Z. *J. Colloid Interface Sci.* **2000**, *221*, 161−165.

(16) Subramanian, V.; Wolf, E. E.; Kamat, P. V. *J. Am. Chem. Soc.* **2004**, *126*, 4943−4950.
(17) Wang, C.; Liu, C.; Zheng, X.; Chen, J.; Shen, T. *Colloids Surf., A***1998**, *131*, 271−280.
(18) Anija, M.; Thomas, J.; Singh, N.; Nair, A. S.; Tom, R. T.; Padeep, T.; Philip, R. *Chem. Phys. Lett.* **2003**, *380*, 223−229.
(19) Tom, R. T.; Nair, A. S.; Singh, N.; Aslam, M.; Nagendra, C. L.; Philip, R.; Vijayamohanan, K.; Pradeep, T. *Langmuir* **2003**, *19*, 3439−3445.
(20) Okumura, M.; Nakamura, S. I.; Tsubota, S.; Nakamura, T.; Haruta, M. *Stud. Surf. Sci. Catal.* **1998**, *118*, 277−284.
(21) Lütt, M.; Fitzsimmons, M. R.; Li, D. *J. Phys. Chem. B* **1998**, *102*, 400−405.
(22) Hattori, H. *Thin Solid Films* **2001**, *385*, 302−306.
(23) Ariga, K.; Lvov, Y.; Ichinose, I.; Kunitake, T. *Appl. Clay Sci.* **1999**, *15*, 137−152.
(24) Claesson, P. M.; Poptoshev, E.; Blomberg, E.; Dedinaite, A. *Adv. Colloid Interface Sci.* **2005**, *114*−*115*,173−187.
(25) Kim, J.; Kim, G.; Cremer, P. *J. Am. Chem. Soc.* **2002**, *124*, 8751−8756.
(26) Horváth, A.; Beck, A.; Sárkány, A.; Guczi, L. *J. Mol. Catal., A* **2002**, *182*−*183*, 295−302.
(27) Schwarz, S.; Buchhammer, H.-M.; Lunkwitz, K.; Jacobasch, H.-J. *Colloids Surf., A* **1998**, *140*, 377−384.
(28) Kekkonen, J.; Stenius, P. *Colloids Surf., A* **1999**, *156*, 357−372.
(29) Möckel, H.; Giersig, M.; Willig, F. *J. Mater. Chem.* **1999**, *9*, 3051−3056.
(30) Baskaran, S.; Song, L.; Liu, J.; Chen, L.; Graff, G. L. *J. Am. Ceram. Soc.* **1998**, *81*, 401−408.
(31) Hanprasopwattana, A.; Rieker, T.; Sault, A. G.; Datye, A. K. *Catal. Lett.* **1997**, *45*, 165−175.
(32) Arpino, P.; Moreau, J.-P.; Oruezabal, C.; Flieder, F. *J. Chromatogr., A* **1977**, *134*, 433−439.
(33) Kreller, D. I.; Gibson, G.; Novak, W.; Van Loon, G. W.; Horton, J. H. *Colloids Surf., A* **2003**, *212*, 249−264.
(34) Su, Z.; Chang, X.; Zhan, G.; Luo, X.; Pu, Q. *Anal. Chim. Acta* 1995, *310*, 493−499.
(35) Xue, L.; Li, Q.; Zhang, Y.; Liu, R.; Hen, X. Z. *J. Eur. Ceram. Soc.* **2006**, *26*, 323−329.
(36) Duan, J.; Gregory, J. *Adv. Colloid Interface Sci.* **2003**, *100*−*102*, 474−502.
(37) Shi, X.; Cassagneau, T.; Caruso, F. *Langmuir* **2002**, *18*, 904−910.
(38) Guo, Y.-G.; Wan, L.-J.; Bai, C.-L. *J. Phys. Chem. B* **2003**, *107*, 5441−5444.
(39) Shutava, T.; Prouty, M.; Kommireddy, D.; Lvov, Y. *Macromolecules* **2005**, *38*, 2850−2858.
(40) Miyazaki, Y.; Shiratori, S. *Thin Solid Films* **2006**, *499*, 29−34.
(41) Srinivasan, S.; Datye, A. K.; Hampden-Smith, M.; Wachs, I. E.; Deo, G.; Jehng, J. M.; Turek, A. M.; Peden, C. H. F. *J. Catal.* **1991**, *131*, 260−275.
(42) Stangland, E. E.; Stavens, K. B.; Andres, R. P.; Delgass, W. N. *J. Catal.* **2000**, *191*, 332−347.
(43) Qi, C.; Akita, T.; Okumura, M.; Haruta, M. *Appl. Catal., A* **2001**, *218*, 81−89.
(44) Chen, Z.; Wang, Z. L.; Zhan, P.; Zhang, J. H.; Zhang, W. Y.; Wang, H. T.; Ming, N. B. *Langmuir* **2004**, *20*, 3042−3046.
(45) Liu, W.; Chen, Y.; Kou, G.; Xu, T.; Sun, D. C. *Wear* **2003**, *254*, 994−1000.
(46) Zhu, J.; Zhang, J.; Chen, F.; Iiono, K.; Anpo, M. *Top. Catal.* **2005**, *35*, 261−268.
(47) Yuan, Z.-Y.; Su, B.-L. *Colloids Surf., A* **2004**, *241*, 173−183.
(48) Tai, Y.; Murakami, J.; Tajiri, K.; Ohashi, F.; Daté, M.; Tsubota, S. *Appl. Catal., A* **2004**, *268*, 183−187.
(49) Gao, X.; Bare, S. R.; Fierro, J. L. G.; Banares, M. A.; Wachs, I. E. *J. Phys. Chem. B* **1998**, *102*, 5653−5666.
(50) Olea, M.; Iwasawa, Y. *Appl. Catal., A* **2004**, *275*, 35−42.
(51) Liu, H.; Kozlov, A. I.; Kozlova, A. P.; Shido, T.; Asakura, K.; Iwasawa, Y. *J. Catal.* **1999**, *185*, 252−264.